Bond Activation by Electron Transfer in Indenyl Ruthenium(II) Complexes. The Electrochemical Reduction of $[Ru(\eta^5\text{-}C_9H_7)Cl(L)_2]$ and $[Ru(\eta^5\text{-}C_9H_7)(L)_2]^+$, L_2 = COD, L = PPh_3[§]

Saverio Santi* and Lorenza Broccardo

Dipartimento di Chimica Fisica, Università degli Studi di Padova, Via Loredan 2, 35131, Padova, Italy

Mauro Bassetti

Istituto CNR di Metodologie Chimiche, and Dipartimento di Chimica, Università "La Sapienza", 00185 Roma, Italy

Patricia Alvarez

Departamento de Química Orgánica e Inorgánica, Instituto de Química Organometálica "Enrique Moles" (Unidad Asociada al CSIC), Facultad de Química, Universidad de Oviedo, 33006 Oviedo, Spain

Received February 5, 2003

The reduction of *half-sandwich* indenyl complexes of general formula $[Ru(\eta^5\text{-}C_9H_7)Cl(L)_2]$ (L = PPh_3, **1**; L_2 = 1,5-cyclooctadiene, **2**) and $[Ru(\eta^5\text{-}C_9H_7)(L)_2]^+$ has been carried out in order to investigate the effects of electron transfer on the structural and chemical properties of the complexes. The reduction of these complexes proceeds by irreversible bielectronic processes. In the case of the metal halide complexes, the first electron transfer generates a 19-electron radical anion, which undergoes Ru−Cl bond cleavage to form a 17-electron $Ru(\eta^5\text{-}C_9H_7)(L)_2$ radical, which is in turn reduced at a less negative potential. Therefore the overall process proceeds according to a ECE mechanism, characterized by two electron transfers separated by a chemical reaction. The cationic $[Ru(\eta^5\text{-}C_9H_7)(L)_2]^+$ complexes were generated in situ by chloride abstraction, upon reacting complex **1** or **2** with $AgBF_4$ or $AgPF_6$; both $[Ru(\eta^5\text{-}C_9H_7)(PPh_3)_2]^+$ (**1a**$^+$) and $[Ru(\eta^5\text{-}C_9H_7)COD]^+$ (**2a**$^+$) undergo a monoelectronic reductive process forming the radical intermediates, which rapidly dimerize. The $[Ru(\eta^5\text{-}C_9H_7)COD]^\bullet$ radical is sufficiently stable to be detected by cyclic voltammetry and partially generates the 18-electron anion $[Ru(\eta^5\text{-}C_9H_7)COD]^-$.

Introduction

Half-sandwich indenyl complexes of transition metals are often characterized by greater reactivity with respect to their cyclopentadienyl analogues, in either stoichiometric[1] or catalytic reactions.[2] This behavior is ascribed to the particular properties of the polyene ligand, which are know as "*indenyl effect*"[3] or "*extra-indenyl effect*".[4] Indenyl complexes of ruthenium(II) have been shown to be active in a variety of chemical processes. Stoichiometric reactions include phosphine substitution as in the case of complex $[Ru(\eta^5\text{-}C_9H_7)Cl(PPh_3)_2]$,[5] insertion of alkynes into the Ru−H bond,[6] and activation of terminal alkynes to form vinylidene and allenylidene complexes.[7] Catalytic processes involve isomerization of allylic alcohols to their saturated aldehydes or ketones,[8] dimerization of terminal alkynes,[9] [2+2] and [2+4] cycloaddition reactions of dienes with alkynes, as in the case of complex $[Ru(\eta^5\text{-}C_9H_7)Cl$-

[§] This paper is dedicated to Prof. Alberto Ceccon on the occasion of his 70th birthday.

* Corresponding author. E-mail: saverio.santi@unipd.it.

(1) Frankom, T. M.; Green, J. C.; Nagy, A.; Kakkar, A. K.; Marder, T. B. *Organometallics* **1993**, *12*, 3688. (b) Rerek, M. E.; Ji, L.-N.; Basolo, F. *J. Chem. Soc., Chem. Commun.* **1983**, 1208. (c) Hart-Davis, A. J.; White, C.; Mawby, R. J. *Inorg. Chim. Acta* **1970**, *4*, 441. (d) Hart-Davis, A. G.; Mawby, R. J. *J. Chem. Soc. A* **1969**, 2403. (e) Jones, D. J.; Mawby, R. J. *Inorg. Chim. Acta* **1972**, *6*, 157.

(2) Borrini A.; Diversi, P.; Ingrosso, G.; Lucherini, A.; Serra, G. *J. Mol. Catal.* **1985**, *30*, 181.

(3) (a) Rerek, M. E.; Basolo, F. *J. Am. Chem. Soc.* **1984**, *106*, 5908. (b) Calhorda M. J.; Veiros, L. F. *Coord. Chem. Rev.* **1999**, *185*−*186*, 37. (c) Basolo, F. *Inorg. Chim. Acta* **1985**, 100, 33. (d) Cheong, M.; Basolo, F. *Organometallics* **1988**, *7*, 2041. (e) Kakkar, A.; Taylor, N. J.; Marder, T. B.; Shen, J. K.; Halliman, N.; Basolo, F. *Inorg. Chim. Acta* **1992**, *219*, 198.

(4) (a) Bonifaci, C.; Carta, G.; Ceccon, A.; Gambaro, A.; Santi, S.; Venzo, A. *Organometallics* **1996**, *15*, 1630. (b) Ceccon, A.; Gambaro, A.; Santi, S.; Venzo, A. *J. Mol. Catal.* **1991**, *69*, L1.

(5) Gamasa, M. P.; Gimeno, J.; Gonzalez-Bernardo, C.; Martín-Vaca, B. M. *Organometallics* **1996**, *15*, 302.

(6) (a) Bassetti, M.; Casellato, P.; Gamasa, M. P.; Gimeno, J.; González-Bernardo, C.; Martín-Vaca, B. *Organometallics* **1997**, *16*, 5470. (b) Bassetti, M.; Marini, S.; Díaz, J.; Gamasa, M. P.; Gimeno, J.; Rodríguez-Álvarez, Y.; García-Granda, S. *Organometallics* **2002**, *21*, 4815.

(7) Cadierno, V.; Gamasa, M. P.; Gimeno, J. *Eur. J. Inorg. Chem.* **2001**, 571.

(8) Trost, B. M.; Kulawiec, R. J. *J. Am. Chem. Soc.* **1993**, *115*, 2027.

(9) Bassetti, M.; Marini, S.; Tortorella, F.; Cadierno, V.; Díez, J.; Gamasa, P. M.; Gimeno, J. *J. Organomet. Chem.* **2000**, 593−594, 292.

10.1021/om0300878 CCC: $25.00
Publication on Web 07/22/2003

(COD)],[10a] and anti-Markovnikov addition of water in aqueous media catalyzed by complex **1**.[11] Despite this extensive chemistry, information about the electrochemical features of these complexes is scarce,[5] as well as about the reactivity of chemically or electrochemically generated species of different oxidation state.

It is known that organometallic radicals with 17 or 19 electrons on the metal generally show greatly enhanced reactivity in comparison to their 18-electron analogues.[12] Electrochemical activation generates more reactive species by raising the ground state energy of the molecules and by altering the energy barrier of the reaction. These species, which can be obtained by photolysis of metal−metal bonded dimeric complexes or by electron transfer on the 18-electron monomers, are frequent intermediates in several organometallic processes, such as atom abstraction, ligand substitution, and disproportionation reactions.[13]

In particular, studies on the redox properties of monomeric metal cyclopentadienyl halides and on their applications as precursors of radical intermediates have been relatively scarce,[14a,15] although more information is available about the corresponding dimeric species.[14] Moreover, despite the high interest in the electron transfer correlated to the indenyl effect,[16] the reductions of indenyl organometallic halides have not been investigated.

In this context we report on the electrochemical reduction of two ruthenium- indenyl complexes illustrated in Scheme 1, viz., [RuCl(η^5-C_9H_7)(PPh_3)$_2$] (**1**) and [RuCl(η^5-C_9H_7)COD] (**2**, COD = 1,5-cyclooctadiene) and of the corresponding cations [Ru(η^5-C_9H_7)(PPh_3)$_2$] (**1**$^+$) and [Ru(η^5-C_9H_7)COD] (**2**$^+$). The bis-phosphine cationic complex **1**$^+$ is the postulated intermediate in the preparation of ruthenium vinylidene complexes from the reaction of terminal alkynes with complex **1**.[7]

Scheme 1

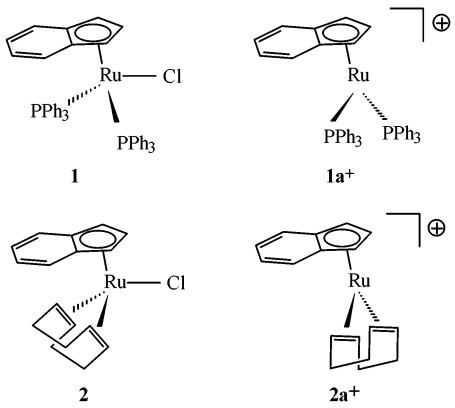

Our aims have been (i) to generate 17- and 19-electron species, (ii) to intercept ruthenium complexes in low oxidation state, and (iii) to identify which bonds are activated by electron transfer. The presence of ligands with different donor properties, such as PPh_3 and COD, affects the electron density on the metal and is therefore expected to influence the electrochemical features of the complexes. Since the stoichiometric and catalytic reactivity strongly depends on the ability to create coordination vacancy at the metal, it is of great interest to assess the structural modifications of the coordination shell induced by electron transfer.

Experimental Section

General Procedures. The complexes [RuCl(η^5-C_9H_7)(PPh_3)$_2$] (**1**)[17] and [RuCl(η^5-C_9H_7)COD][10b,18] (**2**) were prepared according to published procedures. Complexes [Ru(η^5-C_9H_7)(PPh_3)$_2$]$^+$ (**1a**$^+$) and [Ru(η^5-C_9H_7)COD]$^+$ (**2a**$^+$) were prepared in situ, by reacting complex **1** or **2** in THF with an equimolar amount of $AgBF_4$. Electrochemical measurements were performed on clear solutions after removing a pale yellow precipitate by centrifugation. A conductivity measurement (JENWAY PCM 3 conductivity meter) on a THF solution of the cation **2a**$^+$ (1 mM) indicates that the salt behaves as a 1:1 electrolyte (Λ_m =123 Ω^{-1} cm^2 mol^{-1}).

The cationic complex **2a**$^+$ has been fully characterized as the corresponding pyridine or acetonitrile (L) adducts [Ru(η^5-C_9H_7)(L)COD][BF_4].[10a] [Ru(η^5-C_9H_7)(PPh_3)$_2$]$^+$ (**1a**$^+$) has been characterized as hexafluorophosphate salt of the corresponding nitrile adducts [Ru(η^5-C_9H_7)(RCN)(PPh_3)$_2$][PF_6] (R = Me, Et, Ph).[18]

Electrochemical Apparatus and Procedure. All complexes' manipulations were performed in an oxygen- and moisture-free atmosphere; tetrahydrofuran (THF) was purified by distillation from Na/benzophenone under argon atmosphere and then deoxygenated with vacuum line techniques just before use. Ferrocene was purified by crystallization before use. Supporting electrolyte was prepared by exchange reaction of $NaBF_4$ and *n*-Bu_4NHSO_4 in aqueous solution; the precipitate

(10) (a) Alvarez, P.; Gimeno, J.; Lastra, E.; García-Granda, S.; Van der Maelen, J. F.; Bassetti, M. *Organometallics* **2001**, *20*, 3762. (b) Morandini, F.; Consiglio, G.; Sironi, A.; Moret, M. *J. Organomet. Chem.* **1989**, *370*, 305.

(11) Alvarez, P.; Bassetti, M.; Gimeno, J.; Mancini, G. *Tetrahedron Lett.* **2001**, *42*, 8467.

(12) (a) Tyler, D. R. *Acc. Chem. Res.* **1991**, *24*, 325. (b) Therien, M. J.; Ni, C.-L.; Anson, F. C.; Osteryoung, J. G.; Trogler, W. C. *J. Am Chem. Soc.* **1986**, *108*, 4037. (c) Wrighton, M. S.; Ginley, D. S. *J. Am. Chem. Soc.* **1975**, *97*−*98*, 2065. (d) van Raaij, E. U.; Brintzinger, H.-H. *J. Organomet. Chem.* **1988**, *356*, 315. (e) Neto, C. C.; Kim, S.; Meng, Q.; Sweigart, D. A. *J. Am. Chem. Soc.* **1993**, *115*, 2077. (f) Kochi, J. K. *Organometallics Mechanisms and Catalysis*; Academic Press: New York, 1978. (g) Halpern, *J. Pure Appl. Chem.* **1986**, *58*, 575. (h) Bezemo, G. J.; Rieger, P. H.; Visco, S. *J. Chem. Soc., Chem. Commun.* **1981**, 265.

(13) (a) Tyler, D. R. *Prog. Inorg. Chem.* **1988**, *36*, 125. (b) Astruc, D. *Chem. Rev.* **1988**, *88*, 1189. (c) Narayannan B. A.; Amatore, C.; Kochi, J. K. *J. Chem. Soc., Chem. Commun.* **1983**, 397. (d) Kuchynke, D. J.; Amatore, C.; Kochi, J. K. *Inorg. Chem.* **1986**, *25*, 7. (e) *Organometallic Radical Processes*; Trogler, W. C., Ed.; Journal of Organometallic Chemistry Library 22; Elsevier: Amsterdam, 1990. (f) Sun, S.; Sweigart, D. A. In *Advances in Organometallic Chemistry*; Stone, F. G. A., West, R., Eds.; Academic Press: San Diego, CA, 1996; Vol. 40, and references therein.

(14) (a) Marcos, M. L.; Moreno, C.; Macazaga, M. J.; Medina, R.; Maderuelo, R.; Delgado, S.; Gonzalez-Velasco, J. *J. Organomet. Chem.* **1998**, *555*, 57. (b) Tilset, M.; Parker, V. D. *J. Am. Chem. Soc.* **1989**, *111*, 6711. (c) Dalton, E. F.; Ching, S.; Murray, R W. *Inorg. Chem.* **1990**, *30*, 2642. (d) Anderson, J. E.; Liu, Y. H.; Guilard, R.; Barbe, J.-M.; Kadish, K. M. *Inorg. Chem.* **1986**, *25*, 2250. (e) Lacombe, D. A.; Anderson, J. E.; Kadish, K. M. *Inorg. Chem.* **1986**, *25*, 2074.

(15) (a) Teixeira, M. G.; Paolucci, F.; Marcaccio, M.; Aviles, T.; Paradisi, C.; Maran, F.; Roffia, S. *Organometallics* **1998**, *17*, 1297. (b) Weissman, P. M.; Buzzio, D. B.; Wintermute, J. S., Jr. *Microchem. J.* **1981**, *26*, 120. (c) Miholová, D.; Vlcek, A. A. *Inorg. Chim. Acta* **1980**, *43*. (d) Dessy, R. E.; Weissman, P. M. *J. Am. Chem. Soc.* **1966**, *25*, 2250. (e) Gubin, S. P. *Pure Appl. Chem.* **1970**, 23.

(16) (a) Geiger, W. E. *Acc. Chem. Res.* **1995**, *28*, 351. (b) Stoll, M. E.; Belanzoni, P.; Calhorda, M. J.; Drew, M. G. B.; Felix, V.; Geiger, W. E.; Gamelas, C. A.; Gonçalves, I. S.; Romão, C. C.; Veiros L. F. *J. Am. Chem. Soc.* **2001**, *123*, 10595. (c) Amatore, C.; Ceccon, A.; Santi, S.; Verpeaux, J.-N. *Chem.-Eur. J.* **1997**, *3*, 279. (d) Lee, S.; Lovelace, S. R.; Cooper, N. J. *Organometallics* **1995**, *14*, 1974. (e) Miller, G. A.; Therien, M. J.; Trogler, W. C. *J. Organomet. Chem.* **1990**, *383*, 271. (f) Lee, S.; Lovelace, S. R.; Cooper, N. J. *Organometallics* **1995**, *14*, 1974. (g) Wuu, Y. M.; Zou, C. Z.; Wrighton, M. S. *J. Am. Chem. Soc.* **1987**, *109*, 5861.

(17) Oro, L. A.; Ciriano, M. A.; Campo, M.; Foces-Foces, C.; Cano, F. H. *J. Organomet. Chem.* **1985**, *289*, 117.

(18) Cadierno, V.; Gamasa, M. P.; Gimeno, J. *Organometallics* **1999**, *18*, 2821.

was dissolved in CH_2Cl_2, dried with Na_2SO_4, filtered, and dried by evaporation. The salt *n*-Bu_4NBF_4 was then purified by recrystallization from ethyl acetate/petroleum ether. PPh_3 was purified by recrystallization from hexane. COD (Aldrich, 99%) was distilled prior to use. $AgBF_4$, $AgPF_6$ (Aldrich, 99.99%), and Bu_4NCl (Fluka, puriss.) were used without any further purification. Cyclic voltammetry experiments were performed in an airtight three-electrode cell connected to a vacuum/argon line. The reference electrode was a SCE (Taccussel ECS C10) separated from the solution by a bridge compartment filled with the same solvent/supporting electrolyte solution used in the cell. The counter electrode was a platinum spiral with ca. 1 cm^2 apparent surface area. The working electrodes were disks obtained from cross section of gold wires of different diameter (0.5, 0.125, 0.025 mm) sealed in glass. Between each CV scan the working electrode was polished on alumina according to standard procedures and sonicated before use. The currents and potentials were recorded on a Lecroy 9310L oscilloscope. The potentiostat was home-built with a positive feedback loop for compensation of ohmic drop.[19] All potential values are reported versus SCE.

Absolute Electron Stoichiometry Determination.[20] The chronoamperometric diffusion current at 0.5 mm diameter disk electrode for a step duration of 0.2 s and the steady state current at 12.5 μm radius gold microdisk electrode (potential scan rate 10 mV s^{-1}) were measured for 3 mM solutions of **1** and **2** and for the standard ferrocene [$D = (1.3 \pm 0.2) \times 10^{-5}$ cm^2 s^{-1}] under identical conditions, i.e., THF/0.2 M *n*-Bu_4NBF_4. These data allowed determination of the absolute consumption of electrons and of the diffusion coefficients.

Results and Discussion

Electrochemical Reduction of [RuCl(η^5-C_9H_7)-(PPh_3)$_2$] (1). The electrochemical reduction of **1** at 0.5 V s^{-1} (Figure 1a) occurs at $E_p = -1.81$ V as an irreversible process (I) over all the potential scan rates investigated ($v = 0.05-100$ V s^{-1}). After scan reversal, three oxidation waves appear: II ($E_p = -0.52$ V), III ($E_p = 0.29$ V), and IV ($E° = 0.69$ V). The last one is chemically and electrochemically reversible (V). A previous work assigned IV to the one-electron oxidation of complex **1**.[5] II and III are not recorded in the anodic scan, which suggests to ascribe them to the oxidation of species formed in solution after reduction of the complex. At high scan rate (Figure 1b, $v = 200$ V s^{-1}) the wave II has disappeared but the wave III is still present.

The analysis of the reduction wave shows that the current function (i_p $v^{-1/2}$ M^{-1}) changes by varying the scan rate: in fact, it decreases by a factor of 1.7 on going from low scan rate ($v = 0.05$ V s^{-1}) to high scan rate values ($v \geq 10$ V s^{-1}, see Figure 2a). Determination of the absolute electron stoichiometry[20] confirmed that the reduction wave tends to become overall bielectronic at sufficiently low scan rate ($n_{app} = 1.60 \pm 0.15$ at $v \approx 0.1$ V s^{-1}, see Figure 2a). In the general case in which the electron transfer is Nernstian at low scan rate and irreversible at high scan rate, the current function normalized to its value at the highest scan rate is expected to reach the maximum factor of $0.446/0.495(\alpha)^{1/2}$.[21a] The estimated value of $\alpha = 0.54$ (coefficient of the electron transfer) obtained from eq 1, which describes the variation of the peak potential for a totally irreversible electron transfer ($n_\alpha = 1$), justifies a decrease of the current function by a factor 1.22,

$$E_p = (1.15\ RT/\alpha n\alpha F) \log v + \text{constant} \qquad (1)$$

a value definitely less than that observed in our experiments.[21b] This evidence indicates that the experi-

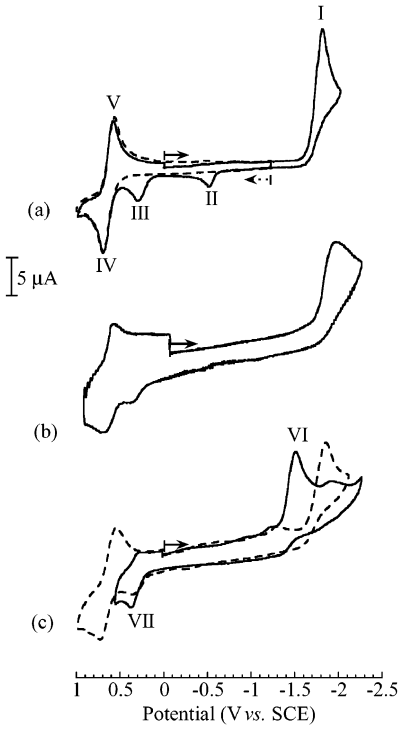

Figure 1. Cyclic voltammetric scans in THF/0.2 M *n*-Bu_4NBF_4 at a gold disk electrode of 0.5 mm diameter, $T = 20$ °C. (a) Reduction (solid line) and oxidation (dotted line) of 3 mM [RuCl(η^5-C_9H_7)(PPh_3)$_2$] (**1**), $v = 0.5$ V s^{-1}; (b) reduction of 3 mM **1**, $v = 200$ V s^{-1}; (c) reduction of 3 mM [Ru(η^5-C_9H_7)(PPh_3)$_2$]$^+$ (**1a**$^+$) (solid line) and after addition of 1 equiv of Bu_4NCl (dotted line), $v = 0.5$ V s^{-1}.

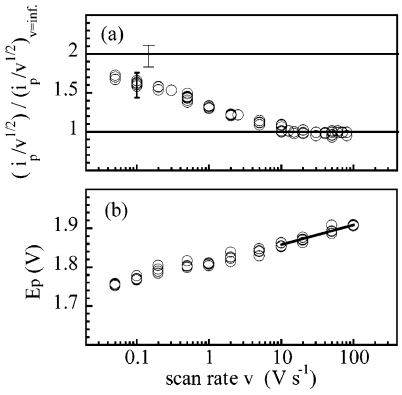

Figure 2. (a) Variation of the current function i_p $v^{-1/2}$ M^{-1} normalized to its value at high scan rate $v \geq 100$ V s^{-1} and (b) variation of the peak potential E_p for the reduction wave of 3 mM [RuCl(η^5-C_9H_7)(PPh_3)$_2$] (**1**) at a gold disk electrode diameter of 0.5 mm, $0.05 \leq v \leq 0.5$, and 0.125 mm, $1 \leq v \leq 100$, $T = 20$ °C. Abscises in logarithmic scale.

(19) Amatore, C.; Lefrou, C.; Pflüger, F. *J. Electroanal. Chem.* **1989**, *43*, 270.

(20) Amatore, C.; Azzabi, M.; Calas, P.; Jutand, A.; Lefrou, C.; Rollin, J. *J. Electroanal. Chem.* **1990**, *288*, 45.

(21) (a) Bard, A. J.; Faulkner, L. R. *Electrochemical Methods*, 2nd. ed.; Wiley: New York, 2001. (b) To verify if the observed trend should be ascribed to a slow electron transfer, we calculated α considering the slope $d(E_p)/d(\log v)$ in the range where the global electronicity remains constant ($v \geq 10$ V s^{-1}, Figure 2b for **1** and 5b for **2**).

mental trend does not depend only on a single and slow electron transfer.

One explanation for the decrease of the current function could be to assume that the reduction of **1** in THF occurs via a CE mechanism in which the chemical step (C) of eq 2 precedes the electron transfer (E) of eq 3, which could occur at sufficiently low scan rate.

$$[RuCl(\eta^5\text{-}C_9H_7)(PPh_3)_2] \underset{k_{-1}}{\overset{k_1}{\rightleftharpoons}} [RuCl(\eta^5\text{-}C_9H_7)(PPh_3)] + PPh_3 \quad (2)$$

$$[RuCl(\eta^5\text{-}C_9H_7)(PPh_3)] + e^- \rightleftharpoons [RuCl(\eta^5\text{-}C_9H_7)(PPh_3)]^- \quad (3)$$

A kinetic study on phosphine substitution for complex **1** in THF has shown the existence of the equilibrium (2) as a step of a dissociative mechanism, in which the release of PPh_3 from ruthenium to form a 16-electron intermediate is rate detemining ($k_1 = 2.04 \times 10^{-4}$ s^{-1}, THF, 30 °C) (eq 2).[5] As far as the reduction mechanism is concerned, the slow rate of the dissociative step reaction k_1 causes the contribution of a CE sequence to become negligible in the global reduction process. In fact, we assessed by digital simulation that such a mechanism would be relevant only for a chemical reaction with $k_1 > 0.01$ s^{-1}.

On the other hand, an ECE mechanism explains the current function shape: the first heterogeneous electron transfer (E) generates an unstable 19-electron species in which a ligand rapidly decoordinates from ruthenium, via loss of Cl^- or PPh_3, or η^5 to η^3 ring-slippage in the chemical step (C). At the electrode−solution interface now exists a 17-electron molecule whose reduction is easier than that of **1**; this species undergoes a second electron transfer (E), generating a bielectronic wave.

To identify the nature of the chemical step, we tested the effect of the complex concentration on the current function and of different amounts of Cl^- and PPh_3. Since no concentration dependence of the current function up to 8 mM **1** was observed, the existence of a second-order chemical reaction involving **1**, such as a disproportionation reaction,[22] can be excluded.

Similar results were obtained from CV experiments at different scan rate carried out on a solution of complex **1** containing up to 10 equiv of PPh_3. The phosphine concentration does not affect the reduction of **1** since no effect is detectable on the current function, and it can be excluded that the chemical reaction is the phosphine dissociation.

In contrast, the addition in solution of similar amounts of *n*-Bu_4NCl causes a decrease of the current function proportional to the concentration of Cl^- (Figure 3a). A common trend is obtained in a plot of $i_p\, v^{-1/2}\, M^{-1}$ versus $\log(v \times C_{Cl^-})$ (Figure 3b), which confirms the presence of a second-order back reaction involving the Cl^- anion.

Concerning the η^5 to η^3 ring-slippage process, it is very typical in 18-electron indenyl complexes[3] and much faster in the corresponding 19-electron radicals.[16] On the basis of the chemical irreversibility of the wave I up to the scan rate investigated ($v = 500$ V s^{-1}) and of the effect of chloride we conclude that the rate-determining chemical step is the chloride dissociation from $[RuCl(\eta^5\text{-}C_9H_7)(PPh_3)_2]^{-\bullet}$ (**1**$^{-\bullet}$), which is retarded by free Cl^- in solution, preceded by a very fast reaction which may be a η^5 to η^3 ring-slippage (eq 5). These results allow the identification of the 17-electron radical $[Ru(\eta^5\text{-}C_9H_7)(PPh_3)_2]^\bullet$ (**1**$^\bullet$) as the species responsible for the second electron transfer at a more positive potential than that of the neutral complex **1**. Equations 4−6 depict the proposed mechanism.

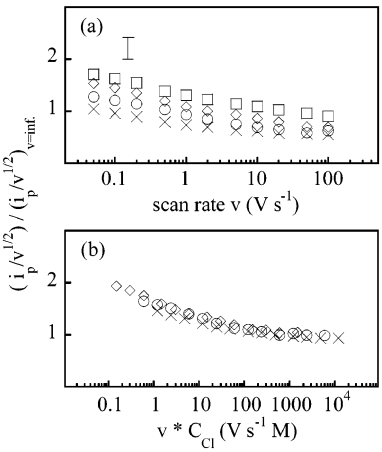

Figure 3. (a) Variation of the current function $i_p\, v^{-1/2}\, M^{-1}$ normalized to its value at high scan rate $v \geq 100$ V s^{-1} of 3 mM $[RuCl(\eta^5\text{-}C_9H_7)(PPh_3)_2]$ (**1**) in the presence of Bu_4NCl, $C_{Cl^-} = 0$ mM (open squares), 3 mM (open diamonds), 12 mM (open circles), and 24 mM (×'s). (b) Variation of the current function obtained in a plot of $i_p\, v^{-1/2}\, M^{-1}$ vs $\log(v \times C_{Cl^-})$. Abscises in logarithmic scale.

At high scan rate, when the wave I is monoelectronic and still irreversible, the intensity of wave III is unchanged (Figure 1b). This indicates that it corresponds to the oxidation of the slipped 17-electron species $RuCl(\eta^3\text{-}C_9H_7)(PPh_3)_2]^{\bullet-}$, which regenerates the starting complex **1**.

$$[RuCl(\eta^5\text{-}C_9H_7)L_2] + e^- \rightleftharpoons [RuCl(\eta^5\text{-}C_9H_7)L_2]^{\bullet-} \quad (4)$$

$$[RuCl(\eta^5\text{-}C_9H_7)L_2]^{\bullet-} \rightarrow [RuCl(\eta^3\text{-}C_9H_7)L_2]^{\bullet-} \rightleftharpoons [Ru(\eta^5\text{-}C_9H_7)L_2]^\bullet + Cl^- \quad (5)$$

$$[Ru(\eta^5\text{-}C_9H_7)L_2]^\bullet + e^- \rightleftharpoons [Ru(\eta^5\text{-}C_9H_7)L_2]^- \quad (6)$$

1: $L_2 = (PPh_3)_2$

2: $L_2 = COD$

Another consequence of the addition of *n*-Bu_4NCl is the decrease of the intensity of II. The wave II is detectable only when the reduction wave of **1** is traversed and disappears at high scan rate ($v \geq 200$ V s^{-1}). It corresponds to the oxidation wave of the indenyl anion,[16c] as demonstrated by comparison with an authentic sample of potassium indenyde and previously observed in analogous experimental conditions for complex $Rh(\eta^5\text{-}C_9H_7)(COD)$. Therefore, it corresponds to the oxidation of the indenyl anion produced by decomposition of **1**$^-$. The intensity of II increases if the scan direction is reversed at more negative potential, i.e., when the chemical reaction has more time to produce

(22) Amatore, C.; Saveant, J. M. *J. Electroanal. Chem.* **1977**, *85*, 27.

the oxidizable species. By this evidence, we conclude that $[Ru(\eta^5\text{-}C_9H_7)(PPh_3)_2]^-$ undergoes a partial degradation which produces the indenyl anion and the fragment $Ru(PPh_3)_2$, which was not detected. The addition of Cl^- in solution inhibits the formation of $[Ru(\eta^5\text{-}C_9H_7)(PPh_3)_2]^-$, and consequently the intensity of wave II decreases due to the indenyl anion.

Electrochemical Reduction of $[Ru(\eta^5\text{-}C_9H_7)(PPh_3)_2]^+$ ($1a^+$). To determine the redox potential of **1a**•, i.e., the key intermediate of the mechanism proposed above, $\mathbf{1a}^+$ was generated inside the electrochemical cell. The CV shows a new chemically irreversible cathodic wave (VI) at −1.5 V, i.e., 310 mV before the peak potential assigned to the reduction of **1** (Figure 1c), which corresponds to the reduction of $\mathbf{1a}^+$. By increasing the scan rate from 0.05 V s^{-1} to 20 V s^{-1}, the current function remains constant, as expected for a process in which the electronicity is unchanged. At the same time, E_p varies linearly with log(v), the slope $d(E_p)/d(\log v)$ being 21 mV, which corresponds, within experimental error, to the value predicted for a radical−radical dimerization (DIM1 mechanism, 19.7 mV).[23] The formation of a new indenyl-containing species after the reduction of the cation is supported by (i) the disappearance of wave II, due to the oxidation of the indenyl anion, and by (ii) the appearance of a new anodic wave VII at $E_p = 0.36$ V. This experimental evidence suggests the formulation of the following DIM1 mechanism for the electrochemical reduction of $[Ru(\eta^5\text{-}C_9H_7)(PPh_3)_2]^+$ (eqs 7, 8):

$$[Ru(\eta^5\text{-}C_9H_7)(PPh_3)_2]^+ + e^- \rightleftharpoons [Ru(\eta^5\text{-}C_9H_7)(PPh_3)_2]^\bullet \quad (7)$$

$$2[Ru(\eta^5\text{-}C_9H_7)(PPh_3)_2]^\bullet \rightleftharpoons [Ru(\eta^5\text{-}C_9H_7)(PPh_3)_2]_2 \quad (8)$$

The 16-electron cation $\mathbf{1a}^+$ undergoes a single electron transfer, generating the radical **1a**• (eq 7), which rapidly dimerizes (eq 8) forming a 34-electron species (wave VII at 0.36 V). Therefore the radical **1a**• dimerizes when produced by reduction of the cation, whereas it is reduced to the anion when formed by chloride dissociation from $\mathbf{1}^{\bullet-}$. This is due to the fact that the radical, in the latter case, is produced at the reduction potential of the neutral complex **1** and is therefore reduced as soon as it is formed. The dimerization process is disfavored since at this potential the redox couple **1a**•/$\mathbf{1a}^-$ can exist only in the reduced form. Alternative dimerization mechanisms involving **1a**• and $\mathbf{1a}^-$ (DIM2), and $\mathbf{1a}^+$ and $\mathbf{1a}^-$ (DIM3), were ruled out on the basis of the slope $d(E_p)/d(\log v)$, which should be 29.6 and 14.8 mV, respectively.[23]

Addition of 1 equiv of n-Bu_4NCl to the solution of the cation restores the starting neutral species, and the waves (I and IV/V) characteristic of **1** are reestablished (Figure 1c).

Electrochemical Reduction of $RuCl(\eta^5\text{-}C_9H_7)$-COD (2). The voltammetric investigation carried out on complex **2** reveals at scan rate $v = 0.5$ V s^{-1} a reduction wave (I) at −1.42 V and, after the scan reversal, four oxidation waves: II ($E_p = -0.90$ V), III ($E_p = 0.43$ V), IV ($E_p = 0.61$ V), and V ($E_p = 1.06$ V), the last one being in part chemically reversible (VI) (Figure 4a). If the anodic scan starts from −1.1 V, only the waves V and its cathodic counterpart VI are detected, indicating that they correspond to the partially reversible oxidation of **2**. Therefore, the wave I represents the reduction of **2**, whereas II, III, and IV correspond to the oxidation of species generated in solution after the reduction of the complex **2**.

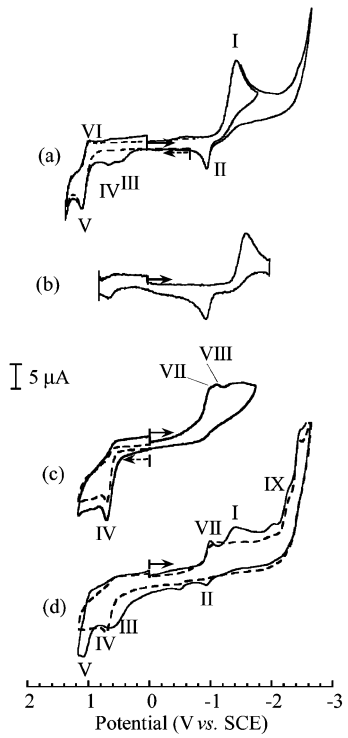

Figure 4. Cyclic voltammetric scans in THF/0.2 M n-Bu_4NBF_4 at a gold disk electrode of 0.5 mm diameter for v = 0.5 V s^{-1}, 0.125 mm for v = 500 V s^{-1}, T = 20 °C. (a) Reduction at $v = 0.5$ V s^{-1} with the potential scan reversed at −1.82 and −2.9 V (solid line) and oxidation (dotted line) of 3 mM $[RuCl(\eta^5\text{-}C_9H_7)COD]$ (**2**); (b) reduction of 3 mM **2** at v = 500 V s^{-1}; (c) reduction (solid line) and oxidation (dotted line) of 3 mM $[Ru(\eta^5\text{-}C_9H_7)COD]^+$ ($\mathbf{2a}^+$); (d) reduction of 3 mM $[Ru(\eta^5\text{-}C_9H_7)COD]^+$ ($\mathbf{2a}^+$) (dotted line) with the potential scan reversed at −2.9 V (dotted line) and after addition of 1 equiv of Bu_4NCl (solid line).

The wave II is present even at high scan rate (v = 500 V s^{-1}, Figure 4b) when the wave I is monoelectronic. Hence, it corresponds to the oxidation of $2^{\bullet-}$ in the scan reversal, demonstrating that reduction of **2** is partially chemically reversible. The current function of the wave I decreases in the range of the scan rate explored (0.05−100 V s^{-1}) (Figure 5a). The value $\alpha = 0.40 \pm 0.01$ allows the prediction of a maximum decrease by a factor 1.42 when the trend is due only to a slow electron transfer.[21] In contrast, the experimental leap is about 1.75, which suggests a more complex mechanism.

Determination of absolute electronic stoichiometry[20] confirms that at low scan rate more than one electron is involved. The value $n_{app} = 1.61 \pm 0.07$ at $v \approx 0.12$ V s^{-1} is in agreement with the current function value at the same scan rate (Figure 5a).

This case also supports the existence of an ECE mechanism in which the chemical step can be either

(23) Andrieux, C. P.; Nadjo, L.; Savéant, J. M. *J. Electroanal. Chem.* **1973**, *42*, 223.

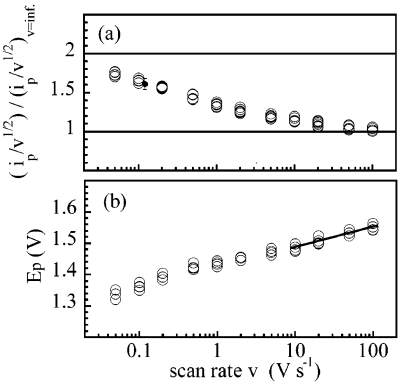

Figure 5. (a) Variation of the current function $i_p\, v^{-1/2}\, M^{-1}$ normalized to its value at high scan rate $v \geq 100$ V s^{-1} and (b) variation of the peak potential E_p for the reduction wave of 3 mM [RuCl(η^5-C_9H_7)COD] (**2**) at a gold disk electrode diameter of 0.5 mm, $0.05 \leq v \leq 0.5$, and 0.125 mm, $1 \leq v \leq 200$, $T = 20$ °C. Abscises in logarithmic scale.

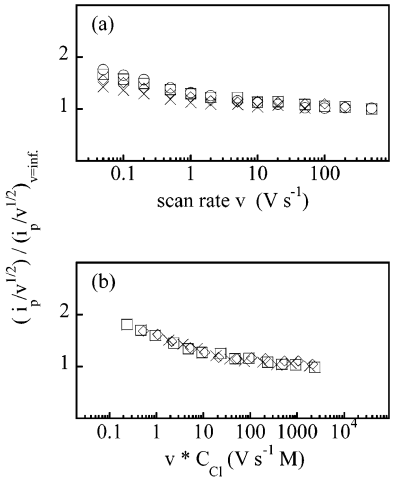

Figure 6. (a) Variation of the current function $i_p\, v^{-1/2}\, M^{-1}$ normalized to its value at high scan rate $v \geq 100$ V s^{-1} of 3 mM [RuCl(η^5-C_9H_7)COD] (**2**) in the presence of Bu_4NCl, $C_{Cl^-} = 0$ mM (open squares), 6 mM (open diamonds), 12 mM (open circles), and 39 mM (×'s). (b) Variation of the current function obtained in a plot of $i_p\, v^{-1/2}\, M^{-1}$ vs $\log(v \times C_{Cl^-})$. Abscises in logarithmic scale.

Ru−Cl or Ru−COD dissociation. No effect was observed, either on the current function or on the voltammogram shape, in the presence of free COD (3−24 mM). On the other hand, the CVs obtained for solutions containing different amounts of *n*-Bu_4NCl showed a decrease of the current function proportional to the concentration of Cl^- (Figure 6a), and a common trend is obtained when $i_p\, v^{-1/2}\, M^{-1}$ is plotted versus $\log(v \times C_{Cl^-})$ (Figure 6b). This indicates that the rate-determining step is the Ru−Cl cleavage, which is retarded when the chloride salt is added in solution, preceded by a η^5 to η^3 ring-slippage, analogous but slower than that occurring at the level of $1^{\bullet-}$ (eq 5) since $2^{\bullet-}$ shows partial chemical reversibility (wave II). These results suggest that the 17-electron radical [Ru(η^5-C_9H_7)(COD)]$^\bullet$ is responsible for the second electron transfer at a more positive potential than the starting complex **2** (eq 6). As in the oxidation of complex **1**, at high scan rate (500 V s^{-1}) the wave III is still present, indicating that it corresponds to the oxidation

Scheme 2

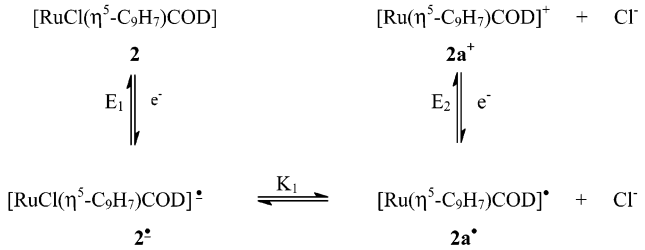

of the slipped 17-electron species RuCl(η^3-C_9H_7)COD]$^{\bullet-}$, which regenerates the neutral complex **2**.

A previous work showed that free COD coordinates [Rh(η^3-η^5-C_9H_7)COD]$^{\bullet-}$ electrochemically generated from Rh(η^5-C_9H_7)COD, producing $C_9H_7^-$ and $Rh(COD)_2$.[16c] In the case of [RuCl(η^5-C_9H_7)COD]$^{\bullet-}$, such a mechanism can be ruled out on the basis of the lack of effects upon addition of free COD.

Electrochemical Reduction of [Ru(η^5-C_9H_7)COD]$^+$ (2a$^+$). The cathodic scan shows two waves of similar potential values (VII, $E_p = -1.01$ V; VIII, $E_p = -1.08$ V), which are 390 mV less negative than that of **2** (Figure 4c). VII can be assigned to the reduction of the 16-electron cation **2a**$^+$ to give the neutral radical **2a**$^\bullet$ via the 17-electron radical Ru(η^5-C_9H_7)COD$^\bullet$. The latter is a 17-electron species, and it is reasonable to suppose that its reduction corresponds to the second wave VIII at more negative potential and the overall reduction of **2a**$^+$ proceeds by two subsequent electron transfers (EE mechanism). The fact that the second peak is not so intense as the first indicates the existence of a chemical reaction which subtracts the radical and at the same time shifts the wave at a more positive potential, close to the first wave, in analogy with what is observed for **1a**$^+$. The formation of new species in solution is supported by the presence of waves at ca. 2.3 V (Figure 4d), which are not observable in the neutral complex. The oxidation wave IV, since it is detected even in the anodic scan (Figure 4c), corresponds to the oxidation of **2a**$^+$. Moreover, by comparison with the cathodic voltammogram at low scan rate in Figure 4a, it is possible to observe that the wave IV is present already before the ionization of **2**, indicating that the cation is formed by oxidation of **2a**$^-$ in the scan reversal after the reduction of **2**.

Addition of 1 equiv of *n*-Bu_4NCl to the solution of the cationic complex causes a better definition of VII, the disappearance of VIII, and the formation of the waves characteristic of the neutral complex (Figure 4d). These results can be explained by the mechanism reported in Scheme 2.

Since the reduction of **2a**$^+$ is still observed even after the addition of *n*-Bu_4NCl, **2a**$^+$ does not react with Cl^-. The equilibrium K_1 is proved by the disappearance of the wave VIII relative to **2a**$^\bullet$, which recombines with Cl^-, generating the radical anion $\mathbf{2}^{\bullet-}$. The latter radical anion is not stable at the potential at which it is formed and hence oxidizes to regenerate the neutral complex **2** and wave I reappears.

Conclusions

This work represents the first report on the electrochemical reduction of indenyl halide complexes and of

the corresponding cationic species obtained by halide abstraction. The study indicates that the electrochemical reduction of both complexes [RuCl(η^5-C_9H_7)(PPh_3)$_2$] (**1**) and [RuCl(η^5-C_9H_7)COD] (**2**) proceeds by an ECE mechanism, in which the chemical step is the Ru−Cl bond dissociation. This bond, under ordinary chemical conditions, can be cleaved only in the presence of strong donor ligands such as PMe_3 or a bidentate chelating phosphine (dppm),[5] or in a solution of strongly coordinating solvents such as acetonitrile and methanol in the presence of $NaPF_6$, or by the action of a precipitating agent (Ag^+).

The reduction of complex **1** and **2** generates the 17-electron radical Ru(η^5-C_9H_7)$L_2^\bullet$ and the corresponding 18-electron anion Ru(η^5-C_9H_7)L_2^-, in which the metal is formally Ru(0). The radical Ru(η^5-C_9H_7)COD$^\bullet$ is sufficiently stable to be observed when generated by reduction of the corresponding cation **2a**$^+$. In fact, the reduction of **2a**$^+$, generated in situ by chloride abstraction, proceeds by two subsequent electron transfers (EE mechanism) via the 17-electron radical Ru(η^5-C_9H_7)-COD$^\bullet$, in which the metal is in the oxidation state I. On the contrary, the analogous radical Ru(η^5-C_9H_7)(PPh_3)$_3^\bullet$ was not detected as intermediate of the reduction of **1a**$^+$ due to a fast radical−radical dimerization via the DIM1 mechanism.

Acknowledgment. This work was supported by the Ministero dell'Università e della Ricerca Scientifica e Tecnologica MURST (COFIN 99, project code 9903198953) and by the CNR (Roma) through its Centro di Studi sugli Stati Molecolari, Radicalici ed Eccitati (Padova).

OM0300878